

Research Article



Tannase Activity Optimization and Antibiotic Resistance Profiling of Bacteria Isolated from Goat Feces and Ruminant Fluid

Nur Farah Syuhada Mohd Zaki¹, Farizan Aris¹, Norfatimah Mohamed Yunus¹, Mohd Taufiq Mat Jalil¹, Nurul Aili Zakaria^{1,2*}

¹Faculty of Applied Sciences, Universiti Teknologi MARA, Shah Alam, Selangor 40450, Malaysia

²Human Genetics and Biochemistry Research Group (Hugeb), Universiti Teknologi MARA, Shah Alam, Selangor 40450, Malaysia

ARTICLE INFO

Article history:

Received February 4, 2025

Received in revised form June 2, 2025

Accepted June 11, 2025

KEYWORDS:

Acinetobacter strain,
Antibiotic resistance,
Lysinibacillus strain,
Optimization,
Tannase,
Tannin-degrading bacteria

ABSTRACT

Tannase is a vital enzyme produced by microorganisms in the rumen and gastrointestinal tracts of animals, capable of converting tannins—a common anti-nutritional factor in feeds. This study optimized physicochemical conditions of pH, temperature, substrate concentration, and incubation time for evaluating crude tannase activity in tannin-degrading bacteria (TDB) isolated from ruminant fluid (TDB17: *Lysinibacillus macroides* (KR780381), TDB18: *Acinetobacter nosocomialis* [MH084921], TDB23: *Acinetobacter nosocomialis* [MT540255]), and goat feces (TDB24: *Acinetobacter nosocomialis* [MT540255]). Among these, TDB23: *A. nosocomialis* (MT540255) demonstrated the highest tannase activity, reaching 96.83 U/ml under optimized conditions. Interestingly, TDB17: *L. macroides* (KR780381) and TDB24: *A. nosocomialis* (MT540255) exhibited thermostable tannase across a temperature between 20°C and 80°C, with sustained activity in the range of 60.15–50.34 U/ml and 29.93–28.98 U/ml, respectively. Additionally, the antibiotic resistance profile of these TDB and the synergistic effects of its crude tannase were evaluated using a disc diffusion assay. All TDBs were susceptible to meropenem, tigecycline, gentamicin, streptomycin, and chloramphenicol but resistant to penicillin G, cephalothin, cefoxitin, and vancomycin. Notably, *A. nosocomialis* (TDB18, TDB23, and TDB24) demonstrated sensitivity to sulfamethoxazole, while *L. macroides* (TDB17) exhibited resistance. Moreover, the crude tannase synergistically enhanced the antibacterial activity of antibiotics ($p < 0.05$) against both Gram-positive and Gram-negative bacteria.



Copyright (c) 2025@ author(s).

1. Introduction

Tannase, or tannin acyl hydrolase, is an enzyme that catalyzes the hydrolysis of ester and depside bonds in hydrolyzable tannins (gallotannins and ellagitannins), complex tannins, and condensed tannins (Hassan *et al.* 2020). These tannins are polyhydroxy phenolic compounds abundantly found in various plants used for food and feed (Mayer 2022). It serves to protect plants against herbivores, pathogenic microbes, and insects (Iqbal and Poór 2024). However, their defensive

mechanisms are nutritionally undesirable due to potential toxicity and interference with nutrient absorption caused by tannin-protein interactions (Hassan *et al.* 2020).

Tannase has been extensively studied since its discovery by Van Tieghem in 1867, with fungal species such as *Aspergillus* sp. and *Penicillium* sp. being prominent tannase producers owing to their robust enzyme production (Aharwar and Parihar 2018; Gezaf *et al.* 2021). Nevertheless, there has been increasing interest in bacterial tannases since 1983, yet reports on them remain scarce in the literature (Belur and Mugeraya 2011). This is because tannin itself is toxic to bacteria due to enzyme inhibition, substrate deprivation, and its activity on the membrane, as well as metal ions

* Corresponding Author

E-mail Address: nurulaili@uitm.edu.my

deficiency (Tahmourespour *et al.* 2016). These factors impede bacterial growth, complicating isolation during the initial stages (Jana *et al.* 2012).

However, a broad spectrum of bacteria in the rumen and gastrointestinal tract of animals can tolerate and degrade tannins through tannase production, as these animals often graze on tannin-rich plants (Tahmourespour *et al.* 2016). These tannin-degrading bacteria (TDB) include genera such as *Bacillus*, *Staphylococcus*, *Klebsiella*, *Lactobacillus*, *Citrobacter*, *Streptococcus*, *Pseudomonas*, *Corynebacterium*, *Pantoea*, *Selenomonas*, *Enterococcus*, and *Serratia* (Mohammed 2016; Tahmourespour *et al.* 2016; Tripathi *et al.* 2016). Bacterial tannase exhibits a high growth rate; however, its optimal production can be significantly influenced by environmental factors such as pH and temperature (Beniwal *et al.* 2014).

Tannase production is typically evaluated through an enzyme activity assay employing a modified spectrophotometric method (de Sena *et al.* 2014). This assay quantifies the hydrolysis of tannic acid by tannase, resulting in the release of gallic acid and glucose (Tang *et al.* 2024). The liberated gallic acid, characterized by vicinal hydroxyl groups, reacts specifically with methanolic rhodanine to form a chromogenic compound, which simultaneously terminates the enzymatic reaction (Sharma *et al.* 2000). Subsequently, potassium hydroxide (KOH) is added to enhance color development. The reaction mixture is diluted with distilled water for absorbance measurement at 520 nm (Chipurura 2010). This method is widely used for routine assessment of tannase activity, offering simplicity, rapid execution, and high reproducibility.

In addition, gallic acid is a major product of tannase activity and exhibits a broad spectrum of pharmacological properties, including antibacterial, antiallergic, antioxidant, antimutagenic, anti-inflammatory, neuroprotective, and anticarcinogenic activities (Selvaraj *et al.* 2022). Considering the emerging threats posed by multiple drug-resistant bacteria, especially Gram-negative species, an alternative approach includes augmenting antimicrobial efficacy with natural inhibitors, such as tannase and gallic acid (Hidayathulla *et al.* 2018). Several studies have reported on the antimicrobial activity of tannin and gallic acid, but there is limited information regarding the antimicrobial resistance profile of TDB and tannase.

Therefore, this study aims to address several key issues by characterizing the properties of crude tannase produced by TDB isolated from ruminal fluid and goat feces using parameters such as pH, substrate

concentration, temperature, and incubation time via modified spectrophotometric methods. Furthermore, their antimicrobial resistance and synergistic effects of tannase were analyzed using commercial antibiotics. It is anticipated that the insights acquired from this study will be utilized across various biotechnological applications, including food processing, bioremediation, poultry feed production, and pharmaceuticals.

2. Materials and Methods

2.1. Enrichment and Reculture of Tannase-Producing Bacteria

Tannase-producing bacterial isolates TDB17, TDB18, TDB23, and TDB24 were obtained from ruminal fluid collected at Kompleks Abatoir Shah Alam and from goat feces at Jariah Agro Farm, Klang. Glycerol stock cultures were initially enriched in nutrient broth supplemented with tannic acid, followed by streaking onto nutrient agar containing tannic acid to promote the selective recovery of tannase-producing bacteria. The resulting colonies were then subcultured onto plain nutrient Agar and incubated overnight at 37°C to rejuvenate the isolates and obtain pure cultures.

2.2. Tannase Activity and Growth Curve of Bacterial Isolate

The production of tannase was prepared using the submerged fermentation (SF) method described by Balakrishnan *et al.* (2021) with minor modifications. The minimal salt medium (MSM) broth was formulated with the following composition (g/L): NH_4Cl , 1.0; KH_2PO_4 , 0.5; MgSO_4 , 0.5; K_2HPO_4 , 0.5; CaCl_2 , 0.1; and addition of 0.6% (w/v) substrate tannic acid. A 500-ml Erlenmeyer flask containing 100 ml of liquid medium was adjusted to pH 5.0±0.2 and sterilized. Then, 1 ml of overnight bacterial culture was inoculated into the prepared MSM broth and fermented for five days in an incubator shaker at 37°C and 180 rpm. Each day, the culture was centrifuged at 4,000 rpm for 10 min at 4°C, and the supernatant was secured as a crude enzyme (Shakir *et al.* 2022). The optical density of the cultures was measured daily at 600 nm until a decline in bacterial growth was noted.

Tannase activity was assessed using a spectrophotometric method described by Srivastava and Kar (2009) with minor modifications. Tannic acid was used as a substrate, and gallic acid as a calibration standard. A 0.5 ml extracted enzyme was added into the substrate in a test tube containing 0.25 ml of 0.01

M tannic acid in 0.05 M citrate buffer with pH 5.0 and incubated at 30°C for 10 min. Next, 0.3 ml of methanolic rhodanine (0.667% w/v Rhodanine in methanol) was added and left for 5 min at room temperature. Thereafter, 0.2 ml of 0.5 M potassium hydroxide solution (KOH) was added, followed by 10 ml of distilled water. The mixture was incubated at 30°C for 10 min, and the purple-pink color formed was measured at 520 nm. The tube for controls was represented by the buffer only, whereas the blank was represented solely by the substrate (Ire and Nwanguma 2020). One unit of tannase activity is defined as the amount of enzyme required to release one μmol of gallic acid formed per minute under certain reaction conditions. Enzyme activity is expressed as U/ml.

2.3. Optimization of Different Physicochemical Parameters of Crude Tannase

The maximum production of crude tannase was characterized under various physicochemical parameters. For each optimization process, the crude enzyme extract was incubated with the substrate in the citrate buffer after the parameters were adjusted. The studied parameters included pH (2.0 to 11.0), substrate concentration (0.2% to 2%), temperature (20 to 80°C), and incubation time (15 minutes to 120 minutes) (Shakir *et al.* 2022). The residual activity was measured using a standard enzyme assay procedure.

2.4. Antibiotic Susceptibility Testing and Synergistic Crude Tannase Effects

The antibiotic susceptibility of TDB was assessed using the disc diffusion method following Clinical Laboratory Standards Institute (CLSI) guidelines. The tested antibiotics included meropenem (MPM 10 μg), penicillin G (PenG 10 μg), chloramphenicol (CHL 30 μg), cephalothin (CFP 30 μg), cefoxitin (CF 30 μg), tigecycline (TIG 15 μg), vancomycin (VA 30 μg), gentamicin (GEN 10 μg), streptomycin (STR 10 μg), and sulfamethoxazole (SXT 25 μg). Standardized bacterial suspensions with an optical density (OD) of 0.08 to 0.1 were swabbed onto the agar plates. Sterile distilled water served as a negative control. The antibiotic discs were then placed onto the plates and incubated overnight at 37°C, after which the zones of inhibition were measured. The antimicrobial and synergistic effects of crude tannase were evaluated against two Gram-positive strains (*Methicillin-resistant Staphylococcus aureus*, *Staphylococcus epidermidis*) and one Gram-negative strain (*Klebsiella pneumoniae*) using the same method. The crude tannase from each TDB was applied to a

blank antibiotic disk and placed on agar plates that were inoculated with the test strains. Citrate buffer was used as a negative control. The synergistic effects were further assessed by combining crude tannase with four (4) antibiotics: (1) meropenem (MPM 10 μg); (2) tigecycline (TIG 15 μg); (3) gentamicin (GEN 10 μg); and (4) streptomycin (STR 10 μg).

3. Results

3.1. Growth Profile and Tannase Activity

The bacterial growth and tannase activity showed a positive correlation with the increasing incubation time, as shown in Figure 1. The exponential growth phase for isolates TDB17 and TDB18 occurred from day 0 to day 3, while for isolates TDB23 and TDB24, it extended from day 0 to day 4. This phase coincided with the highest tannase activity recorded for each isolate: 34.07 U/ml (TDB17), 37.88 U/ml (TDB18), 35.72 U/ml (TDB23) and 42.08 U/ml (TDB24). Following this, the bacterial isolates entered the stationary phase on day 5, which was characterized by a decline in the growth curve and a reduction in enzyme activity.

3.2. Optimization of Different Physicochemical Parameters

The activity of crude tannase was evaluated under varying physicochemical conditions to identify the optimal parameters for maximum enzyme performance. Tannase activity was initiated at pH levels above pH 5 (Figure 2), peaking at pH 6 for TDB18 (45.38 U/ml) and TDB24 (26.96 U/ml). Similarly, the highest tannase activity at pH 7 was recorded for TDB17 (14.46 U/ml) and TDB23 (39.57 U/ml). These results indicate that tannase activity is favored under slightly acidic to neutral conditions, whereas activity declined at higher pH values for all isolates. The analysis of substrate tolerance revealed that all isolates exhibited peak tolerance at a 2% concentration, with TDB17 achieving the highest tannase activity of 69.41 U/ml (Figure 3). Temperature also played a critical role in enzyme activity (Figure 4), with TDB18 exhibiting peak activity (52.60 U/ml) at 30°C, while TDB17 (62.59 U/ml), TDB23 (57.60 U/ml), and TDB24 (38.71 U/ml) showed optimal activities at 40°C. A progressive decline in enzyme activity was noted at higher temperatures. At 80°C, a marked reduction was observed for TDB18 (10.06 U/ml) and TDB23 (4.61 U/ml). Interestingly,

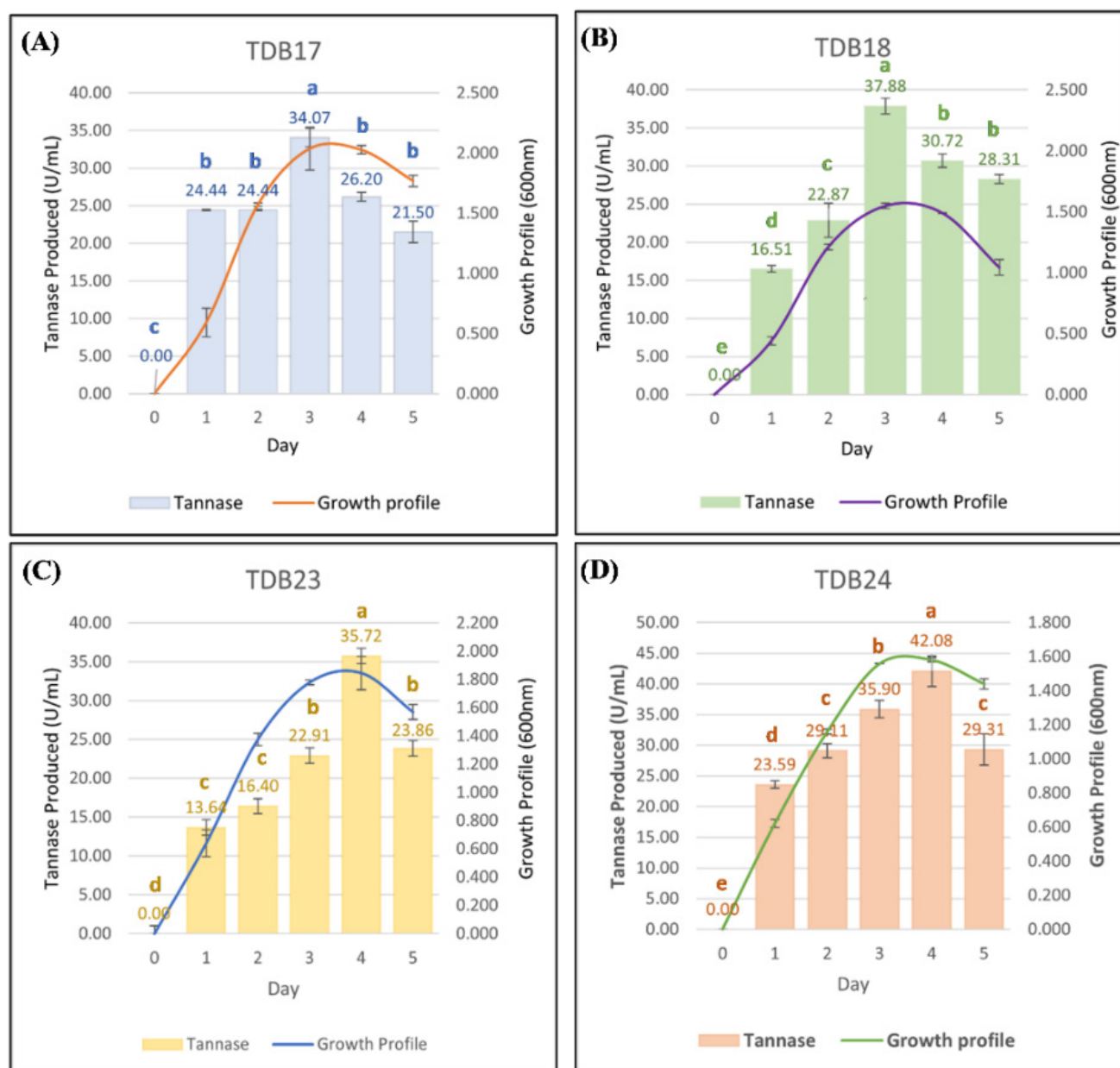


Figure 1. Enzyme activity and bacterial growth of tannin-degrading bacteria (A) TDB17, (B) TDB18, (C) TDB23, and (D) TDB24 over a five-day incubation period. Figures having dissimilar letters differ significantly. (TDB17 = *L. macroides* (KR780381), TDB18, = *A. nosocomialis* (MH084921), TDB23 & TDB24 = *A. nosocomialis* (MT540255))

TDB17 and TDB24 displayed more gradual declines at the same temperature, with activity plateauing at 59.88 U/ml and 28.98 U/ml, respectively. Incubation time significantly influenced tannase activity (Figure 5), remaining stable during the initial 15 minutes and gradually increasing up to 45 minutes. Remarkably, the optimal conditions for the four isolates are summarized in Table 1, with TDB23 (*A. nosocomialis*, MT540255) demonstrating the highest tannase activity, reaching 96.83 U/ml after 45 minutes of incubation under optimized conditions.

3.3. Antibiotic Susceptibility Testing of TDB and Synergistic Crude Tannase Effects

The susceptibility patterns of each bacterium to the standard commercial antibiotics were interpreted in Table 2. The CLSI demonstrated that *L. macroides* (KR780381) and *A. nosocomialis* (MH084921 and MT540255) were susceptible to meropenem (MPM), tigecycline (TIG), gentamicin (GEN), streptomycin (STR), and chloramphenicol (CHL) but resistant to penicillin G (PenG), cephalothin (CFP), cefoxitin (CF), and vancomycin (VA). Notably, *A. nosocomialis*

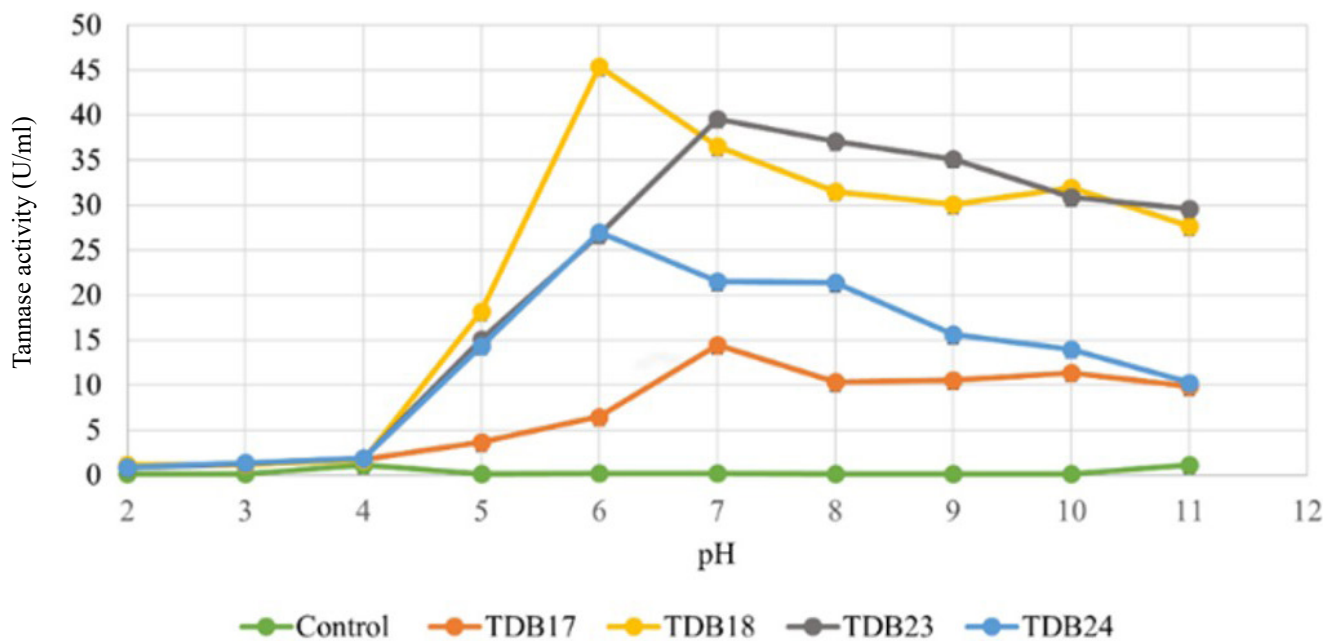


Figure 2. Tannase activity (U/ml) of tannin-degrading bacteria (TDB17, TDB18, TDB23, TDB24) across varying pH levels. (Control: green line = No bacteria, TDB17: orange line = *L. macroides* (KR780381), TDB18: yellow line = *A. nosocomialis* (MH084921), TDB23: grey line & TDB24: blue line = *A. nosocomialis* (MT540255)). Measurements represent mean values from triplicate experiments

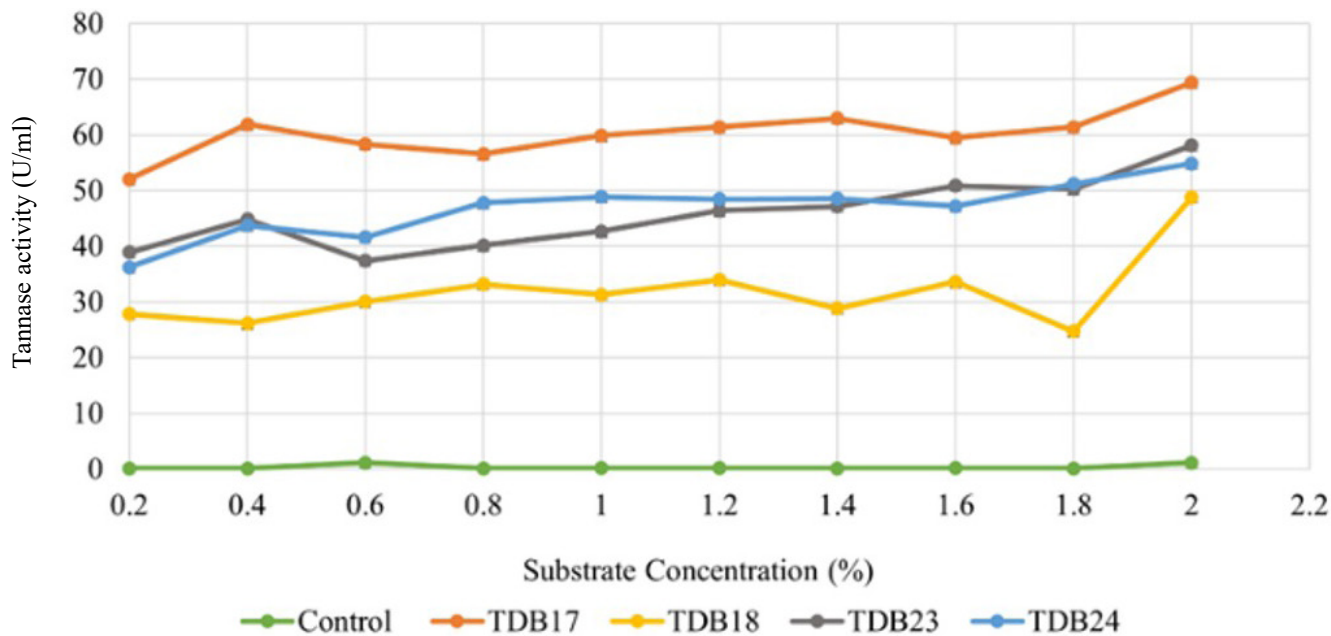


Figure 3. Tannase activity (U/ml) of tannin-degrading bacteria (TDB17, TDB18, TDB23, TDB24) across varying substrate concentrations. (Control: green line = No bacteria, TDB17: orange line = *L. macroides* (KR780381), TDB18: yellow line = *A. nosocomialis* (MH084921), TDB23: grey line & TDB24: blue line = *A. nosocomialis* (MT540255)). Measurements represent mean values from triplicate experiments

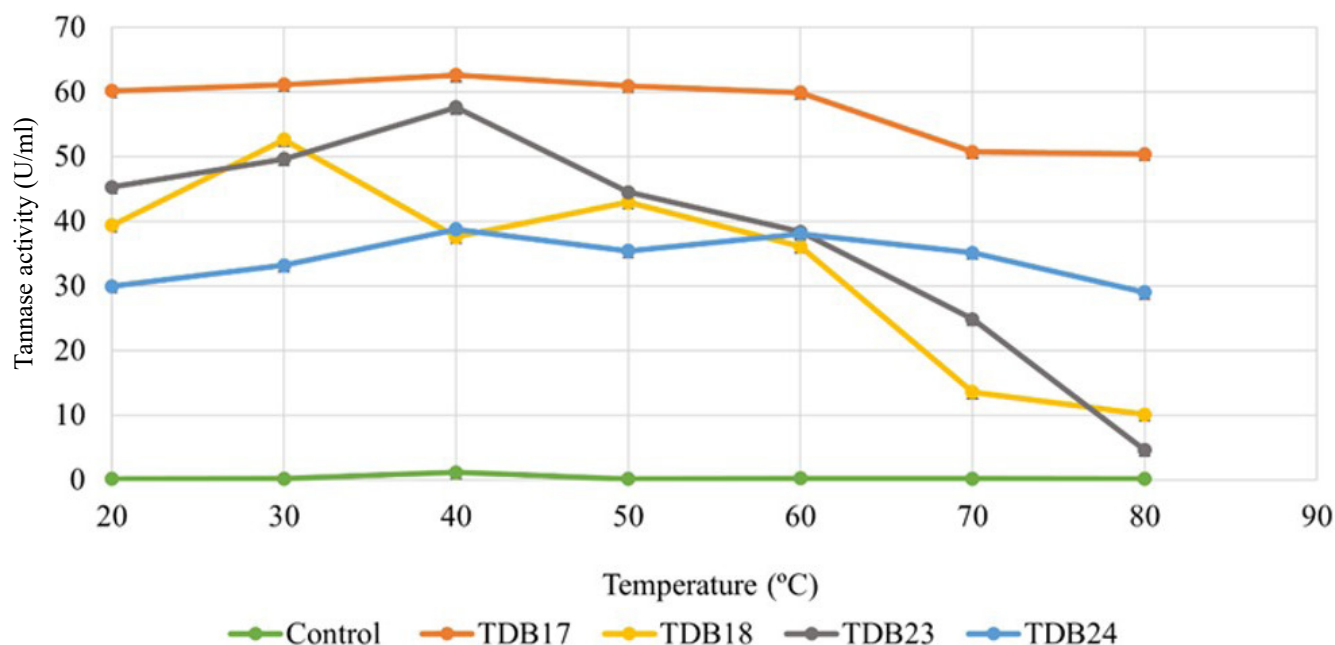


Figure 4. Tannase activity (U/ml) of tannin-degrading bacteria (TDB17, TDB18, TDB23, TDB24) across varying temperature. (Control: green line = No bacteria, TDB17: orange line = *L. macroides* (KR780381), TDB18: yellow line = *A. nosocomialis* (MH084921), TDB23: grey line & TDB24: blue line = *A. nosocomialis* (MT540255)). Measurements represent mean values from triplicate experiments

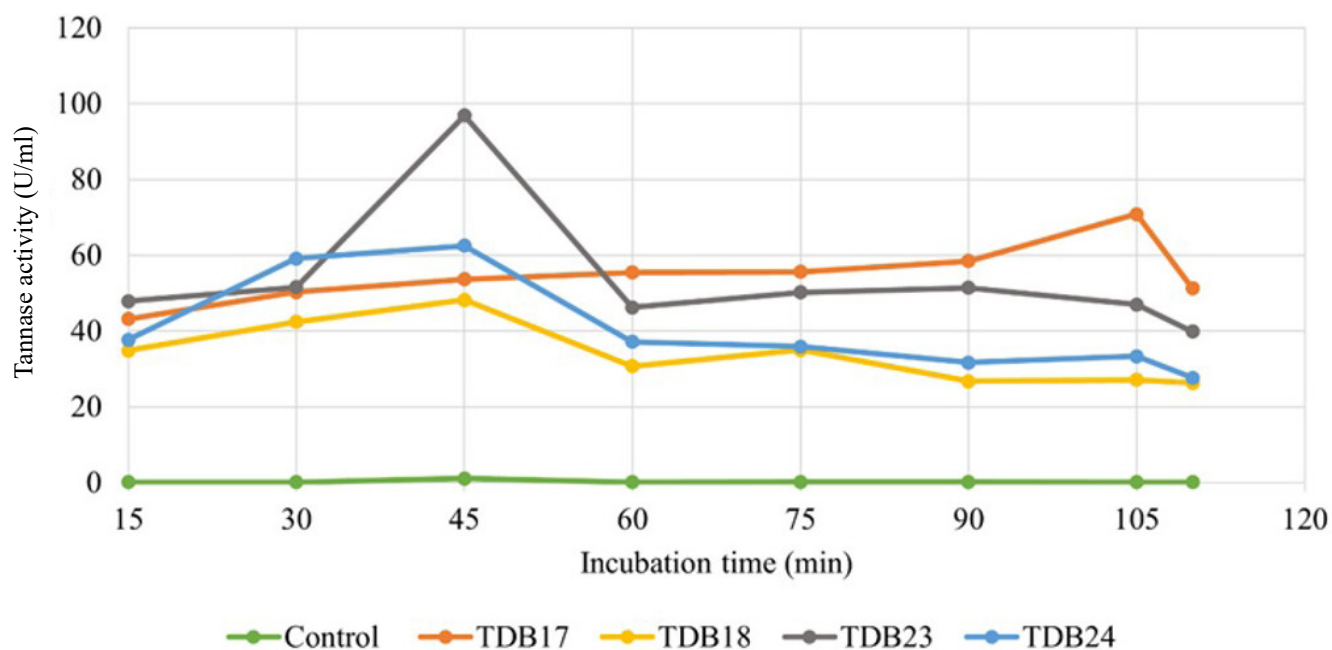


Figure 5. Tannase activity (U/ml) of tannin-degrading bacteria (TDB17, TDB18, TDB23, TDB24) across varying incubation time. (Control: green line = No bacteria, TDB17: orange line = *L. macroides* (KR780381), TDB18: yellow line = *A. nosocomialis* (MH084921), TDB23: grey line & TDB24: blue line = *A. nosocomialis* (MT540255)). Measurements represent mean values from triplicate experiments

Table 1. Optimal fermentation condition for each isolate in tannase production by submerged fermentation

Optimization condition of MSM supplemented with Tannic acid		TDB17 <i>Lysinibacillus macrolides</i> (KR780381)	TDB18 <i>Acinetobacter nosocomialis</i> (MH084921)	TDB23 <i>Acinetobacter nosocomialis</i> (MT540255)	TDB24 <i>Acinetobacter nosocomialis</i> (MT540255)
pH	Optimal	7	6	7	6
	Tannase activity	14.46 U/ml	45.38 U/ml	39.57 U/ml	26.96 U/ml
Substrate concentration	Optimal	2%	2%	2%	2%
	Tannase activity	69.41 U/ml	48.77 U/ml	58.15 U/ml	54.86 U/ml
Temperature	Optimal	40°C	30°C	40°C	40°C
	Stability	20-80°C	20-60°C	20-60°C	20-80°C
	Tannase activity	60.15-50.34 U/ml	39.35-36.03 U/ml	45.28-38.31 U/ml	29.93-28.98 U/ml
Incubation time	Optimal	105 min	45 min	45 min	45 min
	Tannase activity	70.85 U/ml	48.19 U/ml	96.83 U/ml	62.51 U/ml
Fold increment		2.08	1.27	2.71	1.49

Data represent the optimal conditions and corresponding tannase activity for each bacterial strain under minimal salt medium (MSM) supplemented with tannic acid. Tannase activity is reported in U/ml

Table 2. Means of inhibition zones (mm) of each isolated tannin-degrading bacteria against 10 types of antibiotics

Commercial antibiotics	Means of inhibition zones of standard antibiotics discs against tested bacterial strains (mm)			
	TDB17 <i>L. macrolides</i> (KR780381)	TDB18 <i>A. nosocomialis</i> (MH084921)	TDB23 <i>A. nosocomialis</i> (MT540255)	TDB24 <i>A. nosocomialis</i> (MT540255)
Meropenem (10 mcg)	S (27.22±1.72)**	S (28.22±1.48)**	S (28.11±1.27)**	S (26.78±1.48)**
Penicillin G (10 iU)	R (8.89±2.03)*	R (11.78±3.35)*	R (9.44±2.13)*	R (12.33±1.32)*
Chloramphenicol (30 mcg)	I (14.56±3.71)*	I (12.78±2.91)*	I (15.78±3.90)*	I (11.11±2.47)*
Cephalothin (30 mcg)	R (0±0)	R (0±0)	R (0±0)	R (0±0)
Cefoxitin (30 mcg)	R (13.22±1.56)*	R (16.67±2.35)*	R (13.11±1.36)*	R (13.78±0.97)*
Tigecycline (15 µg)	S (27.67±1.80)*	S (22.22±0.67)*	S (23.22±0.67)*	S (24.78±0.83)*
Vancomycin (30 µg)	R (9.44±0.53)*	R (0±0)	R (0±0)	R (0±0)
Gentamicin (10 µg)	S (22.33±1.80)*	S (14.89±0.78)*	S (18.78±0.44)*	S (18.78±0.93)*
Streptomycin (10 µg)	S (27.78±1.99)*	S (21.78±1.30)*	S (22.11±0.93)*	S (23.89±0.93)*
Sulfamethoxazole (25 µg)	R (7.89±5.97)*	S (16.33±1.12)*	S (17.22±1.92)*	S (19.00±1.00)*

R = Resistant; I = Intermediate; S = Susceptible

* - Significant (p<0.05); ** - Insignificant (p>0.05)

± indicates standard deviation

The inhibition zone for each bacterium was analyzed according to the CLSI Standard

(TDB18, TDB23, and TDB24) demonstrated sensitivity to sulfamethoxazole (SXT), while *L. macrolides* (TDB17) exhibited resistance.

The effects of crude tannase from four isolates, alone and in combination with antibiotics, revealed distinct inhibitory patterns against the tested strains (Table 3). Crude tannase alone from each strain exhibited antibacterial activity only against *S.*

epidermidis, with a 9 mm inhibition zone. Notably, the combination of crude tannase and antibiotics enhanced the inhibitory effect on most bacterial strains, demonstrating a synergistic effect. The highest activity was observed against MRSA when combined with gentamicin, producing inhibition zones ranging from 9±0.0 to 12±2.9 mm, with fold area increases of 1.25 (TDB17), 1.01 (TDB18), 2.78 (TDB23), and

Table 3. Synergistic activity of crude tannase and antibiotics against MRSA, *K. pneumoniae* and *S. epidermidis*

Extract from isolate	Test strains	Mean inhibition zone (mm) of antibiotic discs in combination with the crude tannase against clinical bacterial strains ¹												
		CT	GEN	GEN + CT	Fold area ²	S	S + CT	Fold area ²	MEM	MEM + CT	Fold area ²	TGC	TGC + CT	Fold area ²
TDB17	MRSA	0	0	9±0.0	1.25	12±0.6	13±0.8	0.20	0	6±0.5	0.00	23±0.8	28±1.2	0.41
	<i>K. pneumoniae</i>	0	23±1.7	25±1.0	0.17	23±1.2	25±1.2	0.16	0	9±0.4	1.25	21±1.9	24±0.8	0.23
	<i>S. epidermidis</i>	9	30±3.5	33±3.3	0.25	0	8±1.3	0.70	0	12±0.5	3.23	28±0.8	31±0.5	0.20
TDB18	MRSA	0	0	9±0.5	1.01	12±1.5	13±1.4	0.03	0	6±0.8	0.00	25±4.0	29±2.8	0.27
	<i>K. pneumoniae</i>	0	23±2.6	25±1.3	0.23	24±2.0	25±1.8	0.03	0	8±0.5	0.93	22±1.5	24±1.4	0.16
	<i>S. epidermidis</i>	9	31±5.3	36±1.1	0.33	0	10±1.1	1.78	0	9±0.4	1.17	27±0.5	30±2.0	0.31
TDB23	MRSA	0	0	12±2.9	2.78	13±0	15±0.5	0.24	0	6±0.4	0.00	26±2.4	29±1.6	0.22
	<i>K. pneumoniae</i>	0	23±1.0	24±1.6	0.15	22±1.2	25±0.5	0.22	0	8±1.1	0.78	22±0.8	25±0.8	0.24
	<i>S. epidermidis</i>	9	34±0.8	35±0	0.04	0	10±0.8	1.51	0	8±1.0	0.85	27±0.5	31±2.4	0.35
TDB24	MRSA	0	0	10±1.3	1.87	14±1.6	15±2.8	0.15	0	7±0.5	0.49	23±4.1	27±3.5	0.43
	<i>K. pneumoniae</i>	0	24±1.0	26±0.9	0.22	22±0.5	24±1.8	0.18	0	8±0.8	0.85	22±1.2	24±0.5	0.16
	<i>S. epidermidis</i>	9	32±3.1	37±2.2	0.32	0	9±0	1.25	0	8±1.0	0.85	28±1.0	30±1.0	0.12

CT – Crude Tannase; GEN – Gentamicin (10 µg); S – Streptomycin (30 µg); MEM – Meropenem (10 µg); TGC – Tigecycline (25 µg)

¹Mean surface area of the inhibition zone was calculated for each from the mean diameter

²Increase in fold area was calculated as $= (y^2 - x^2) / x^2$, where 'x' and 'y' are the inhibition zones for antibiotic and antibiotic + tannase, respectively

*In the absence of bacterial growth inhibition zones, the disk's diameter (6 mm) was used to calculate the fold increases

Red – Resistant; Blue – Susceptible

± indicates standard deviation

1.87 (TDB24). Similarly, the four isolates displayed maximum activity with the combination of crude tannase with meropenem against *K. pneumoniae*, demonstrating inhibition zones in ranges of 6±0.4 to 12±0.5 mm and fold areas of 0.78 to 1.25. Meanwhile, the combination of crude tannase from TDB17 with meropenem showed the highest fold area at 3.23 against *S. epidermidis* with an inhibition zone increasing from 0 to 12±0.5 mm. In contrast, the crude tannase of TDB18, TDB23, and TDB24 demonstrated the highest activity in combination with streptomycin against *S. epidermidis*, resulting in fold area increases of 1.78, 1.51, and 1.25, respectively.

4. Discussion

The use of submerged fermentation (SF) enhances tannase production by providing high water content, which improves nutrient solubility and accessibility to bacterial cells, resulting in more efficient substrate utilization (Singh and Jana 2023). Besides, SF allows for better control of parameters to optimize bacterial growth and cultivation (Aharwar and Parihar 2018). Many tannase-producing microorganisms require slightly acidic to alkaline conditions and specific temperatures to optimize enzyme activity (Aguilar-Zarate *et al.* 2015; Kumar *et al.* 2019; Mohapatra *et al.*

2020; Unban *et al.* 2020; Dhiman *et al.* 2021; Shakir *et al.* 2022).

In this study, four bacterial strains were isolated from ruminal fluid (TDB17: *Lysinibacillus macroides* (KR780381), TDB18: *Acinetobacter nosocomialis* (MH084921), and TDB23: *Acinetobacter nosocomialis* (MT540255)) and goat feces (TDB24: *Acinetobacter nosocomialis* (MT540255)) demonstrated positive tannin degradation capabilities in the preliminary screening by a previous study (Suhaimi *et al.* 2024). These strains are capable of producing tannase enzymes that comprise two isoenzymes responsible for depsidase and esterase activities (Mancheño *et al.* 2022). Tannase sequentially hydrolyzes tannic acid by first cleaving the depside bond, followed by the hydrolysis of ester bonds, yielding glucose and gallic acid (GA) through intermediates such as 2,3,4,6-tetragalloyl glucose and two forms of monogalloyl glucose (Govindarajan *et al.* 2016). GA is then decarboxylated into pyrogallol, which is further metabolized into metabolites such as pyruvic acid cis-aconitic acid (3-hydroxy-5-oxo-hexanoate) and ultimately enters the TCA cycle (Gauri *et al.* 2013). Yet the complete pathway remains only partially understood.

The growth profiles and tannase activities can vary among bacterial strains, with *Bacillus* species generally exhibiting peak enzyme activity between days 1 and 3.

For instance, *B. licheniformis*, isolated from Iraqi soil, produced a maximum tannase activity of 76.8 U/ml at 72 hours (Jebur 2020), while *B. megaterium* demonstrated its highest activity of 10.77 U/ml/min during the same period (Tripathi *et al.* 2016). Conversely, *B. velezensis* TA3, isolated from saltpan soil samples, reached its peak activity of 2U/g on day 2 before subsequently declining (Lekshmi *et al.* 2020), whereas *B. gottheilii* M2S2, recovered from tannery effluent soil, exhibited optimal activity on day 1 (Subbalaxmi and Murthy 2016). Furthermore, Abdulshaheed *et al.* (2023) reported that the *Acinetobacter baumannii* yielded the highest tannase activity, reaching 26.46 mg/ml after 72 hours. This peak activity corresponds to the exponential growth phase, characterized by rapid bacterial cell division (Jebur 2020). The following decrease in enzyme activity was attributed to nutrient depletion, which led to a higher rate of cell death, thereby reducing enzyme synthesis (Jebur 2020).

According to Leangnim *et al.* (2023), most bacterial tannases are denatured at low pH but exhibit optimal activity between pH 4.0 to 7.0, aligning with the findings of this study. Given the limited data on tannase activity in the newly reported *Lysinibacillus* genus, a comparative analysis was conducted with the *Bacillus* genus since both belong to the Firmicutes family. The optimal tannase activity observed at pH 7 in *Lysinibacillus* corresponds with that of *B. amyloliquefaciens*, which exhibited 6 U/ml at the same pH (Shakir *et al.* 2022). However, several *Bacillus* species isolated from soil, including *B. subtilis*, *B. licheniformis*, and *B. gottheilii*, displayed ideal tannase activity at pH 5 (Aftab and Hamid 2016; Subbalaxmi and Murthy 2016; Jebur 2020), while others such as *B. sphaericus*, *B. megaterium*, and *B. subtilis* showed peak activity at pH 6 (Raghuwanshi *et al.* 2011; Tripathi *et al.* 2016; Sharba *et al.* 2022). Notably, *B. subtilis* isolated from the gut of *Catla catla* fish exhibited a maximum tannase activity of 218.38 U/ml at an alkaline pH of 8 (Shakir *et al.* 2022). Meanwhile, *A. nosocomialis* (MH084921 and MT540255) produced optimal tannase activity at pH 6 to 7, whereas *A. baumannii* showed a peak at pH 5.5 (Abdulshaheed *et al.* 2023). However, the capability of *Acinetobacter* spp. as a tannase producer was only discovered in 2021 by Mohammadabadi *et al.* (2021); hence, no detailed information has been provided. Yet, the decline in tannase activity at both lower and higher pH levels in this study may be attributed to pH-induced modifications of carboxyl and amino groups on the enzyme surfaces, leading to enzyme inactivation

and, consequently, a reduction in both its synthesis and catalytic activity (Shakir *et al.* 2022). Additionally, the formation of tannic acid salts under alkaline conditions may reduce substrate availability, further limiting enzymatic action (Jebur 2020).

In terms of substrate concentration, the findings of this study align with previous reports identifying 2% tannic acid as optimal for tannase activity in free-cell form (Jebur 2020). Likewise, *B. sphaericus* showed maximum tannase production (11.2 IU/ml) at 2.0% tannic acid (Raghuwanshi *et al.* 2011), while other *Bacillus* genera optimized at concentrations ranging from 0.5 to 2.5% (Dhiman *et al.* 2021; Shakir *et al.* 2022). In addition, *B. subtilis* achieved the highest reported activity at 211.97 U/ml using 4.0% tannic acid in combination with 0.5% MgSO₄ and 1.5% yeast extract (Shakir *et al.* 2022). Although data on the effect of substrate concentration in *Acinetobacter* was limited, Abdulshaheed *et al.* (2023) revealed tannase production by *A. baumannii* at a 0.5% concentration. The present findings suggest that *Lysinibacillus* sp. (KR780381) and *Acinetobacter* sp. (MH084921 and MT540255) may tolerate higher tannic acid concentrations. Yet, tannic acid can be toxic to microbes due to its elevated phenolic content, which can precipitate macromolecules like proteins and carbohydrates, thereby impeding microbial growth and inhibiting tannase activity (Mohapatra *et al.* 2020). Moreover, increased substrate levels can reduce tannase activity due to the accumulation of intermediate hydrolysates and gallic acid, which can competitively or non-competitively bind to the active sites of the enzyme, blocking its function (Patil *et al.* 2011; Selvaraj and Murty 2017). Consequently, evaluating higher tannic acid concentrations is essential to ascertain its toxicity range to bacteria and identify the optimal concentration for microbial tannase biosynthesis.

The results on tannase activity at varying temperatures align with existing literature, which indicates that most bacterial tannases exhibit optimal activity between 30°C and 40°C (Shakir *et al.* 2022). For instance, tannase from *B. gottheilii* M2S2 displayed peak activity (49.32 U⁻¹) at 32°C (Subbalaxmi and Murthy 2016), and *B. licheniformis* exhibited optimal production at 35°C, reaching 64.14 U/ml (Jebur 2020). Similarly, tannase activity shown by *A. baumannii* is optimal at 37°C (Abdulshaheed *et al.* 2023). A further increase in temperature resulted in decreased tannase activity for most strains, likely due to excessive potential energy disrupting weak bonds in the enzyme's

structure, leading to denaturation, loss of structural integrity, and inactivation of both the enzymes, as well as the substrates (Cavalcanti *et al.* 2018). Yet, TDB17 and TDB24 could be potential sources of thermostable tannase, as they remain fairly active up to 80°C without significant loss of activity. This is an additional advantage given that most of the processes assisted by tannase are performed at higher temperatures. While reports on tannase production at higher temperatures are limited, Beniwal *et al.* (2014) believed that bacteria are also resilient to extreme temperatures. Aftab and Hamid (2016) reported tannase synthesis with rising temperature, with maximal observed at 41°C for *B. subtilis*. Additionally, Govindarajan *et al.* (2019) reported optimal tannase production from *Enterobacter cloacae* strain 41 at 50°C, yielding 2.418 U/ml.

On top of that, incubation time is essential for assessing the stability interaction between tannic acid and crude tannase under optimized conditions, ensuring sufficient catalysis for converting to gallic acid. Shakir *et al.* (2022) reported that *B. subtilis* showed maximum tannase activity after 30 minutes (233.34 U/ml), and *Raoultella ornithinolytica* exhibited peak activity at 60 minutes (194.07 U/ml). These findings highlight the variability in tannase stability among bacterial strains over time. As incubation progresses, crude tannase activity tends to decline, likely due to enzyme denaturation or structural instability under prolonged exposure, even in optimized conditions (Govindarajan *et al.* 2019; Jebur 2020). This underscores the importance of determining the optimal incubation duration to maintain enzyme efficacy for bioconversion processes. Thus, tannic acid commonly presents challenges in microbial studies due to its inhibitory effects on growth and metabolism. Initial cultures were grown on nutrient-rich media, such as nutrient agar supplemented with low concentrations of tannic acid, to mitigate inhibition and prevent nutrient imbalance or depletion. The use of commercial tannic acid in the rhodanine assay resulted in high absorbance, likely due to gallic acid impurities; hence, a tannic acid blank was included for accurate measurement.

In this antibiotic profiling, *L. macroides* (KR780381) and *A. nosocomialis* (MH084921 and MT540255) exhibited resistance to cell wall synthesis antibiotics, including penicillin G (PenG), cephalothin (CFP), cefoxitin (CFX) and vancomycin (VA). These antibiotics are β -lactam antibiotics, except for vancomycin, which belongs to the glycopeptide antibiotic. This resistance pattern observed aligns with

previous reports indicating that *L. macroides* (Byayika *et al.* 2022) and *Acinetobacter* sp. (Barnes *et al.* 2019) can produce β -lactamase enzymes that hydrolyze the β -lactam ring, a critical structure in β -lactam antibiotics, thereby preventing these antibiotics from binding to the bacterial penicillin-binding proteins (PBPs). Nevertheless, Sun *et al.* (2020) reported susceptibility to vancomycin, which contrasts with the current findings that confirm acquired resistance in *L. macroides* as mentioned by Byayika *et al.* (2022), raising concerns over potential horizontal gene transfer to other bacteria amid limited data on antibiotic effects in *Lysinibacillus* species. Moreover, vancomycin is ineffective against Gram-negative bacteria, such as *A. baumannii*, due to their impermeable outer membrane to large glycopeptide molecules (Kyriakidis *et al.* 2021). Since both *A. nosocomialis* (MH084921 and MT540255) and *L. macroides* (KR780381) produced β -lactamases, they remain susceptible to meropenem, as it is not broken down by these enzymes (Dhillon 2018).

Meanwhile, both strains showed susceptibility to all antibiotics within the protein synthesis inhibitor class, such as tigecycline (TIG), gentamicin (GEN), streptomycin (STR), and chloramphenicol (CHL), though each operates via distinct mechanisms. This suggests that they do not carry transferable AMR genes for protein synthesis inhibitors. Inggraini *et al.* (2021) reported the resistance of *A. baumannii* to aminoglycosides and tigecycline, which contradicts the results of this study. The only *L. macroides* (KR780381) exhibited resistance to sulfamethoxazole that may arise from genetic alterations affecting protein affinity, plasmid or chromosomal genes causing mutations in DHPS and DHFR, cross-resistance and excessive para-aminobenzoic acid (PABA) production, cell wall alterations and increased dihydrofolate reductase production (Uddin *et al.* 2021). However, limited data on the effects of various antibiotics on both bacteria suggest that organic acid may be the main compound responsible for the observed inhibition. Therefore, further research is essential to explore the underlying mechanisms and fill the knowledge gaps regarding the antimicrobial profiles of these strains.

As far as we know, this is the first study to characterize the antibacterial activities of tannase derived from bacterial species. The synergistic activity of tannase together with antibiotics has been aligned with the previous study by Hidayathulla *et al.* (2018) and Kang *et al.* (2018) against *Streptococcus agalactiae*,

Staphylococcus aureus, *Pseudomonas aeruginosa*, *Shigella flexneri*, and *Klebsiella pneumonia*, resulting in lower MIC and increased diameter of inhibition. Moreover, Abdulshaheed *et al.* (2023) reported that purified tannase alone isolated from *A. baumannii* displayed a zone of inhibition towards *E. coli*, *E. cloacae*, *K. pneumoniae*, *S. marcescens*, *P. aeruginosa*, and *S. aureus* ranging from 20 to 30 mm. The mechanisms underlying tannase's synergistic effect with antibiotics have not been fully elucidated. Still, previous studies by Hidayathulla *et al.* (2018) suggested that it may involve inhibition of bacterial surface attachment or interruption of Quorum Sensing (QS). Observations demonstrated from their study that the inclusion of tannase with antibiotics enhances effectiveness against bacteria and inhibits biofilm formation in multiple bacterial strains, indicating the potential of tannase as a new antibacterial agent. The combined action of tannase with antibiotics, such as streptomycin and ceftazidime, highlights its efficacy in fighting bacteria, offering strong antibacterial and anti-biofilm properties. This finding highlights the antibacterial properties of tannase and its potential as a novel antibacterial agent.

Moreover, the outcomes of this work also revealed that the GA may have contributed to the synergistic effect since the extracted tannase was not purified. Borges *et al.* (2013) demonstrated the antibacterial activity of GA against strains such as *E. coli*, *P. aeruginosa*, *S. aureus*, and *Listeria monocytogenes*, causing membrane pores and led to irreversible changes by altering membrane permeability, hydrophobicity, and physicochemical properties. A study by Lu *et al.* (2021) showed that GA exhibited strong antibacterial activity against Methicillin-Sensitive *S. aureus* (MSSA) and Methicillin-resistant *S. aureus* (MRSA) by disrupting membrane adhesions and increasing membrane permeability, leading to elevated bacterial fluid conductivity. Nevertheless, Rajamanickam *et al.* (2019) revealed that GA also enhances the effectiveness of antibacterial compounds like ciprofloxacin, erythromycin, norfloxacin, oxacillin, ampicillin, gentamicin, and penicillin through synergistic interactions. Considering the widespread resistance of bacteria to existing antibiotics, combination therapy becomes crucial for increased efficacy in existing antibiotics and reduces the spread of drug resistance (Buchmann *et al.* 2022). Hossain *et al.* (2020) investigated the combined effect of GA with traditional antibiotics (Thiamphenicol) on *E. coli*, finding synergistic effects. Thus, future studies could further investigate the mechanisms of action

and explore the clinical applications of this synergistic approach in antibacterial therapy.

In conclusion, this study is the first to report the characterization and antibiotic resistance profiles of four tannase-producing bacteria isolated from ruminal fluid and goat feces. Among these, *A. nosocomialis* strain MT540255 (TDB23) emerged as the most efficient tannase producer, exhibiting the highest activity of 96.83 U/ml under optimal conditions. In addition, *L. macroides* strain KR780381 (TDB17), and *A. nosocomialis* strain MT540255 (TDB24) demonstrated thermostable tannase activity, maintaining 50.34-62.59 U/ml at temperatures up to 80°C. Collectively, these features highlight their potential for diverse industrial enzyme applications. In terms of antibiotic susceptibility, *A. nosocomialis* was sensitive to sulfamethoxazole, whereas *L. macroides* was resistant. Importantly, all strains showed significant synergistic effects when combined with antibiotics, suggesting an opportunity for therapeutic studies. Future research should focus on optimizing crude tannase by exploring the effects of oxygen tension, agitation speed, additives, and nutrient sources to maximize its activity. This may reveal the capability of tannin-degrading bacteria for biotechnological uses, especially in bioremediation and poultry feed production. Moreover, purifying tannase is recommended to enhance its stability and efficiency. It facilitates detailed studies of its structure, activity, and antibiotic interactions, thereby promoting understanding of its antimicrobial properties and pharmaceutical prospects.

Acknowledgements

Authors acknowledge the Universiti Teknologi MARA for funding under the Geran Penyelidikan MyRA (600-RMC 5/3GPM (037/2023).

References

- Abdulshaheed, A.A., Hanafiah, M.M., Muslim, S.N., 2023. Screening and optimization of a novel gallic acid and tannase production under semi-quantitative and quantitative methods. *IOP Conf. Ser.: Earth Environ. Sci.* 1167, 012046. <http://doi.org/10.1088/1755-1315/1167/1/012046>
- Aftab, M.N., Hamid, M., 2016. Production and characterization of tannase from a newly isolated *Bacillus subtilis*. *Pak. J. Bot.* 48, 1263- 1271.
- Aguilar-Zarate, P., Cruz, M.A., Montañez, J., Rodriguez-Herrera, R., Wong-Paz, J. E., Belmares, R. E., Aguilar, C. N., 2015. Gallic acid production under anaerobic submerged fermentation by two bacilli strains. *Microb. Cell Fact.* 4, 1-7. <https://doi.org/10.1186/s12934-015-0386-2>

- Aharwar, A., Parihar, D.K., 2018. Tannases: production, properties, applications. *Biocatal. Agric. Biotechnol.* 15, 322-334. <https://doi.org/10.1016/j.bcab.2018.07.005>
- Balakrishnan, A., Kanchinadham, S.B.K., Kalyanaraman, C., 2021. Studies on the effect of bacterial tannase supplementation to biodegradation of tannins in tannery wastewater. *Ind. Eng. Chem. Res.* 60, 16854-16863. <https://doi.org/10.1021/acs.iecr.1c02987>
- Barnes, M.D., Kumar, V., Bethel, C.R., Moussa, S.H., O'Donnell, J., Rutter, J.D., Good, C.E., Bonomo, R.A., 2019. Targeting multidrug-resistant *Acinetobacter* spp.: sulbactam and the diazabicyclooctenone β -lactamase inhibitor ETX2514 as a novel therapeutic agent. *MBio.* 10, 10.1128/mbio.00159-19. <https://doi.org/10.1128/mbio.00159-19>
- Belur, P.D., Mugeraya, G., 2011. Microbial production of tannase: state of the art. *Res. J. Microbiol.* 6, 25-40.
- Beniwal, V., Kumar, R., Kumari, A., Chhokar, V., 2014. Microbial production of tannase in Microbes in The Service of Mankind. pp. 463-488.
- Borges, A., Ferreira, C., Saavedra, M.J., Simões, M., 2013. Antibacterial activity and mode of action of ferulic and gallic acids against pathogenic bacteria. *Microb Drug Resist.* 19, 256-265. <https://doi.org/10.1089/mdr.2012.0244>
- Buchmann, D., Schultze, N., Borchardt, J., Böttcher, I., Schaufler, K., and Guenther, S., 2022. Synergistic antimicrobial activities of epigallocatechin gallate, myricetin, daidzein, gallic acid, epicatechin, 3-hydroxy-6-methoxyflavone and genistein combined with antibiotics against ESKAPE pathogens. *J. Appl. Microbiol.* 132, 949-963. <https://doi.org/10.1111/jam.15253>
- Byakika, S., Mukisa, I.M., Muyanja, C., 2022. Lactic acid bacteria antagonism of acid tolerant and antibiotic resistant non-*Staphylococcal* pathogenic species isolated from a fermented cereal beverage using baird parker agar. *Nutr. Food Sci. Res.* 9, 31-40. <http://doi.org/10.52547/nfsr.9.1.31>
- Cavalcanti, R.M.F., Jorge, J.A., Guimarães, L.H.S., 2018. Characterization of *Aspergillus fumigatus* CAS-21 tannase with potential for propyl gallate synthesis and treatment of tannery effluent from leather industry. *3 Biotech.* 8, 1-11. <https://doi.org/10.1007/s13205-018-1294-z>
- Chipurura, B., 2010. Nutritional content, phenolic compounds composition, and antioxidant activities of selected indigenous vegetables of Zimbabwe [Thesis]. Harare, Zimbabwe: University of Zimbabwe.
- de Sena, A.R., Dos Santos, A.C.D.B., Gouveia, M.J., de Mello, M.R.F., Leite, T.C.C., Moreira, K.A., de Assis, S.A., 2014. Production, characterization and application of a thermostable tannase from *Pestalotiopsis guepinii* URM 7114. *Food Technol Biotechnol.* 52, 459. <https://doi.org/10.17113/ftb.52.04.14.3743>
- Dhillon, S., 2018. Meropenem/vaborbactam: a review in complicated urinary tract infections. *Drugs.* 78, 1259-1270. <https://doi.org/10.1007/s40265-018-0966-7>
- Dhiman, S., Mukherjee, G., Kumar, A., Majumdar, R.S., 2021. Enhanced production of tannase through RSM by *Bacillus haynesii* SSRY4 MN031245 under submerged fermentation. *J. Sci. Ind. Res.* 80, 675-680. <https://doi.org/10.56042/jsir.v80i08.39264>
- Gauri, S.S., Mandal, S.M., Atta, S., Dey, S., Pati, B.R., 2013. Novel route of tannic acid biotransformation and their effect on major biopolymer synthesis in *Azotobacter* sp. SSB81. *J. Appl. Microbiol.* 114, 84-95. <https://doi.org/10.1111/jam.12030>
- Gezaf, S.A., Abo Nouh, F.A., Abdel-Azeem, A.M., 2021. Fungal communities from different habitats for tannins in industry, in: Abdel-Azeem, A.M., Yadav, A.N., Yadav, N., Sharma, M. (Eds.), *Industrially Important Fungi for Sustainable Development. Fungal Biology*. Springer, Cham, pp. 153-176. http://doi.org/10.1007/978-3-030-85603-8_4
- Govindarajan, R.K., Revathi, S., Rameshkumar, N., Krishnan, M., Kayalvizhi, N., 2016. Microbial tannase: current perspectives and biotechnological advances. *Biocatal. Agri. Biotechnol.* 6, 168-175. <https://doi.org/10.1016/j.bcab.2016.03.011>
- Govindarajan, R.K., Krishnamurthy, M., Neelamegam, R., Shyu, D.J., Muthukalingan, K., Nagarajan, K., 2019. Purification, structural characterization and biotechnological potential of tannase enzyme produced by *Enterobacter cloacae* strain 41. *Process Biochem.* 77, 37-47. <https://doi.org/10.1016/j.procbio.2018.10.013>
- Hassan, Z.M., Manyelo, T. G., Selaledi, L., and Mabelebele, M., 2020. The effects of tannins in monogastric animals with special reference to alternative feed ingredients. *Molecules.* 25, 4680. <https://doi.org/10.3390/molecules25204680>
- Hidayathulla, S., Shahat, A.A., Alsaid, M.S., Al-Mishari, A.A., 2018. Optimization of physicochemical parameters of tannase post-purification and its versatile bioactivity. *FEMS Microbiol. Lett.* 365, fny051. <https://doi.org/10.1093/femsle/fny051>
- Hossain, M.A., Park, H.C., Lee, K.J., Park, S.W., Park, S.C., Kang, J., 2020. In vitro synergistic potentials of novel antibacterial combination therapies against *Salmonella enterica* serovar Typhimurium. *BMC Microbiol.* 20, 1-14. <https://doi.org/10.1186/s12866-020-01810-x>
- Inggraini, M., Nurfajriah, S., Priyanto, J.A., Ilsan, N.A., 2021. Antimicrobial susceptibility and molecular species identification of clinical carbapenem resistant bacteria. *BioloDiversitas.* 22, 555-562. <https://doi.org/10.13057/biodiv/d220206>
- Iqbal, N., Poór, P., 2024. Plant protection by tannins depends on defence-related phytohormones. *J. Plant Growth Regul.* 44, 22-39. <https://doi.org/10.1007/s00344-024-11291-1>
- Ire, F.S., Nwanguma, A.C., 2020. Comparative evaluation on tannase production by *Lasiodiplodia plurivora* ACN-10 under submerged fermentation (SmF) and solid-state fermentation (SSF). *Asian J Biotechnol. Bioresour. Technol.* 6, 39-49. <http://doi.org/10.9734/ajb2t/2020/v6i130074>
- Jana, A., Maity, C., Halder, S.K., Pati, B. R., Mondal, K. C., Mohapatra, P. K., 2012. Rapid screening of tannase producing microbes by using natural tannin. *Braz. J. Microbiol.* 43, 1080-1083. <https://doi.org/10.1590/S1517-838220120003000034>
- Jebur, H.A., 2020. Optimization of production and partial purification of tannase from local isolate of *Bacillus licheniformis* HJ2020 MT1417. *Plant Archives.* 20, 2963-2968.
- Kang, J., Liu, L., Liu, M., Wu, X., Li, J., 2018. Antibacterial activity of gallic acid against *Shigella flexneri* and its effect on biofilm formation by repressing mdoH gene expression. *Food Control.* 94, 147-154. <https://doi.org/10.1016/j.foodcont.2018.07.011>
- Kumar, M., Rajesh, V.S., Salar, R.K., 2019. Upgradation of tannase production by *Klebsiella pneumoniae* KP715242 through heat, UV, NTG and MMS induced mutagenesis for enhanced tannase activity. *Biosc. Biotech. Res. Comm.* 12, 128-134. <http://doi.org/10.21786/bbrc/12.1/15>
- Kyriakidis, I., Vasileiou, E., Pana, Z.D., and Tragiannidis, A., 2021. *Acinetobacter baumannii* antibiotic resistance mechanisms. *Pathogens.* 10, 373. <https://doi.org/10.3390/pathogens10030373>
- Leangnim, N., Unban, K., Thangsunan, P., Tateing, S., Khanongnuch, C., Kanpiengjai, A., 2023. Ultrasonic-assisted enzymatic improvement of polyphenol content, antioxidant potential, and in vitro inhibitory effect on digestive enzymes of Miang extracts. *Ultrason Sonochem.* 94, 106351. <https://doi.org/10.1016/j.ultsonch.2023.106351>
- Lekshmi, R., Nisha, S.A., Kaleeswaran, B., Alfharhan, A.H., 2020. Pomegranate peel is a low-cost substrate for the production of tannase by *Bacillus velezensis* TA3 under solid state fermentation. *J. King Saud Univ. Sci.* 32, 1831-1837. <https://doi.org/10.1016/j.jksus.2020.01.022>
- Lu, L., Zhao, Y., Yi, G., Li, M., Liao, L., Yang, C., Cheng, Q., 2021. Quinic acid: A potential antibiofilm agent against clinical resistant *Pseudomonas aeruginosa*. *Chin. Med.* 16, 1-17. <https://doi.org/10.1186/s13020-021-00481-8>

- Mancheño, J. M., Atondo, E., Tomás-Cortázar, J., Luís Lavín, J., Plaza-Vinuesa, L., Martín-Ruiz, I., Barriales, D., Palacios, A., Navo, C. D., Sampedro, L., Peña Cearra, A., Pascual-Itoiz, M. A., Castelo, J., Carreras-González, A., Castellana, D., Pellón, A., Delgado, Susana., Ruas-Madiedo, P., de las Rivas, B., Abecia, L., Muñoz, R., Jiménez-Osés, G., Anguita, J., Rodríguez, H., 2022. A structurally unique *Fusobacterium nucleatum* tannase provides detoxicant activity against gallotannins and pathogen resistance. *Microb Biotechnol.* 15, 648-667. <https://doi.org/10.1111/1751-7915.13732>
- Mayer, F., 2022. Tanins: natural plant-derived polyhydroxy phenolic compounds with potential for biotechnological and biomedical applications. *WJBPHS.* 2, 1-4. <https://doi.org/10.53346/wjbpr.2022.2.1.0127>
- Mohammadabadi, T., Gheibipour, M., Motamedi, H., Chaji, M., Abbas, B.A., 2021. Isolation and identification of tannin-degrading bacteria from deer gut and potency for improving nutritional value of tannin rich plants. *J. Iran. Vet.* 17, 65-75. <http://dx.doi.org/10.22055/IVJ.2021.257994.2322>
- Mohammed, Y.H.I., 2016. Isolation and characterization of tannic acid hydrolysing bacteria from soil. *Biochem. Anal. Biochem.* 5, 254-260. <http://doi.org/10.4172/2161-1009.1000254>
- Mohapatra, P.K.D., Biswas, I., Mondal, K.C., Pati, B.R., 2020. Concomitant yield optimization of tannase and gallic acid by *Bacillus licheniformis* KBR6 through submerged fermentation: an industrial approach. *Acta Biol. Szeged.* 64, 151-158. <http://doi.org/10.14232/abs.2020.2.151-158>
- Patil, D.B., Das, S.K., Das Mohapatra, P.K. Nag, A., 2011. Physico-chemical studies and optimization of gallic acid production from the seed coat of *Terminalia belerica* Roxb. *Annals Microbiol.* 61, 649-654. <https://doi.org/10.1007/s13213-010-0185-2>
- Raghuwanshi, S., Dutt, K., Gupta, P., Misra, S., Saxena, R. K., 2011. *Bacillus sphaericus*: the highest bacterial tannase producer with potential for gallic acid synthesis. *J. Biosci. Bioeng.* 111, 635-640. <https://doi.org/10.1016/j.jbiosc.2011.02.008>
- Rajamanickam, K., Yang, J., Saktharkar, M.K., 2019. Gallic acid potentiates the antimicrobial activity of tulathromycin against two key bovine respiratory disease (BRD) causing-pathogens. *Front. Pharmacol.* 9, 1486. <https://doi.org/10.3389/fphar.2018.01486>
- Selvaraj, S., Amaral, J.M., Murty, V.R., 2022. Kinetics and antimicrobial activity of gallic acid by novel bacterial co-culture system using Taguchi's method and submerged fermentation. *Arch. Microbiol.* 204, 584. <https://doi.org/10.1007/s00203-022-03168-2>
- Selvaraj, S., Murty, V., 2017. Semi-solid state fermentation: a promising method for production and optimization of tannase from *Bacillus gottheilii* M2S2. *Res J. Biotech.* 12, 4.
- Shakir, H.A., Javed, I., Irfan, M., Ali, S., Khan, M., Qazi, J.I., Yousaf, M.A., 2022. Tannase production from *Bacillus amyloliquefaciens* in submerged fermentation through response surface methodology: tannase production from *Bacillus amyloliquefaciens*. *Biological Sciences-PJSIR.* 65, 95-103. <https://doi.org/10.52763.PJSIR.BIOL.SCI.65.2.2022.95.103>
- Sharba, M.M., Mohammed, A.A., Mohammed, S.F., 2022. Isolation and characterization of tannase from isolated *Bacillus subtilis*. *YMER.* 21, 766-776.
- Sharma, S., Bhat, T.K., Dawra, R.K., 2000. A spectrophotometric method for assay of tannase using rhodanine. *Anal. Biochem.* 279, 85-89. <https://doi.org/10.1006/abio.1999.4405>
- Singh, B., Jana, A.K., 2023. Agri-residues and agro-industrial waste substrates bioconversion by fungal cultures to biocatalyst lipase for green chemistry: a review. *J. Environ. Manage.* 348, 119219. <https://doi.org/10.1016/j.jenvman.2023.119219>
- Srivastava, A., Kar, R., 2009. Characterization and application of tannase produced by *Aspergillus niger* ITCC 6514.07 on pomegranate rind. *Braz. J. Microbiol.* 40, 782-789. <https://doi.org/10.1590/s1517-83822009000400008>
- Subbalaxmi, S., Murty, V.R., 2016. Process optimization for tannase production by *Bacillus gottheilii* M2S2 on inert polyurethane foam support. *Biocatal. Agric. Biotechnol.* 7, 48-55. <https://doi.org/10.1016/j.cbab.2016.05.004>
- Suhaimi, M.S., Zailani, F.A., Mohd Zaki, N.F.S., Aris, F., Mat Jalil, M.T., Zakaria, N.A., 2024. Isolation and identification of tannin-degrading bacteria from goat feces, ruminal fluid, and rumen gut. *MAB Journal.* 53, 23-37. <https://doi.org/10.55230/mabjournal.v53i3.2999>
- Sun, H., Bjerketorp, J., Levenfors, J.J., Schnürer, A., 2020. Isolation of antibiotic-resistant bacteria in biogas digestate and their susceptibility to antibiotics. *Environ. Pollut.* 266, 115265. <https://doi.org/10.1016/j.envpol.2020.115265>
- Tahmourespour, A., Tabatabaee, N., Khalkhali, H., Amini, I., 2016. Tannic acid degradation by *Klebsiella* strains isolated from goat feces. *Iran. J. Microbiol.* 8, 14.
- Tang, Z., Shi, L., Liang, S., Yin, J., Dong, W., Zou, C., Xu, Y., 2024. Recent advances of tannase: production, characterization, purification, and application in the tea industry. *Foods.* 14, 79. <https://doi.org/10.3390/foods14010079>
- Tripathi, A.D., Sharma, A.B.L., Lakshmi, B., 2016. Study on tannase producing *Bacillus megaterium* isolated from tannery effluent. *Int. J. Adv. Res. Biol. Sci.* 3, 28-35. <http://doi.org/1.15/ijarbs-2016-3-7-5>
- Uddin, T.M., Chakraborty, A.J., Khushro, A., Zidan, B.R.M., Mitra, S., Emran, T.B., Koirala, N., 2021. Antibiotic resistance in microbes: history, mechanisms, therapeutic strategies and future prospects. *J. Infect. Public Health.* 14, 1750-1766. <https://doi.org/10.1016/j.jiph.2021.10.020>
- Unban, K., Kodchasee, P., Shetty, K., Khanongnuch, C., 2020. Tannin-tolerant and extracellular tannase producing *Bacillus* isolated from traditional fermented tea leaves and their probiotic functional properties. *Foods.* 9, 490. <https://doi.org/10.3390/foods9040490>